Spectroscopy of the Fractional Vortex Eigenfrequency in a Long Josephson 0-κ Junction

K. Buckenmaier,[1] T. Gaber,[1] M. Siegel,[2] D. Koelle,[1] R. Kleiner,[1] and E. Goldobin[1,*]

[1]*Physikalisches Institut–Experimentalphysik II, Universität Tübingen, Auf der Morgenstelle 14, D-72076 Tübingen, Germany*
[2]*Universität Karlsruhe, Institut für Mikro–und Nanoelektronische Systeme, Hertzstraße 16, D-76187 Karlsruhe, Germany*

(Received 2 October 2006; published 15 March 2007)

Fractional Josephson vortices carry a magnetic flux Φ, which is a fraction of the magnetic flux quantum $\Phi_0 \approx 2.07 \times 10^{-15}$ Wb. Their properties are very different from the properties of the usual integer fluxons. In particular, fractional vortices in 0-κ Josephson junctions are pinned and have an oscillation eigenfrequency which is expected to be within the Josephson plasma gap. Using microwave spectroscopy, we investigate the dependence of the eigenfrequency of a fractional Josephson vortex on its magnetic flux Φ and on the bias current. The experimental results are in good agreement with the theory.

DOI: 10.1103/PhysRevLett.98.117006 PACS numbers: 74.50.+r, 05.45.−a, 74.20.Rp, 85.25.Cp

Vortices in long Josephson junctions (LJJs) usually carry a single magnetic flux quantum Φ_0 and therefore are called fluxons. The study of fluxons has attracted a lot of attention during the last 40 years because of their interesting nonlinear nature [1–3] as well as because of potential applications [4,5].

Recently, it turned out that one can create and study experimentally vortices that carry only a *fraction* of the magnetic flux quantum [6]. Initially, vortices carrying only $\Phi_0/2$ (semifluxons) were observed and studied [9–11]. They exist in the so-called 0-π LJJs [12–14] consisting of 0-parts, having the usual current-phase relation (CPR) $j_s = j_c \sin(\mu)$, and π-parts, having negative critical current or, equivalently, the CPR shifted by π, i.e., $j_s = -j_c \sin(\mu) = j_c \sin(\mu - \pi)$. Here j_s and j_c are the supercurrent and the critical current densities and μ is the Josephson phase. 0-π LJJs can be fabricated using various technologies, e.g., based on d-wave superconductors [9–11,15] or on a ferromagnetic barrier [16–18].

In contrast to a fluxon, which is a freely moving soliton, a semifluxon is like a spin-$\frac{1}{2}$ particle—it is pinned at a 0-π boundary and has two possible polarities $\pm\frac{1}{2}\Phi_0$. Semifluxons are very interesting nonlinear objects: they can form a variety of groundstates [19–22], may flip [9,10] emitting a fluxon [21,23,24], or rearrange [25] by a bias current. Huge arrays of semifluxons were realized [10] and predicted to behave as tunable photonic crystals [26]. Semifluxons can also be used for storage of classical information and to build qubits [27].

From the above CPRs it is clear that one can always describe the supercurrent flowing across the whole LJJ as $j_s = j_c \sin(\phi)$ with the phase $\phi(x)$ being π-*discontinuous* at the boundaries between the 0 and π regions. In essence, a semifluxon appears to compensate this discontinuity and to minimize the total energy. Using an artificial trick with two tiny current injectors, we suggested creating not only π, but any *arbitrary* κ discontinuity of the phase, i.e., a so-called 0-κ LJJ. Thus, one can study the arbitrary $-\kappa$ vortex [carrying the flux $\Phi = -\Phi_0\kappa/(2\pi)$], which automatically appears to compensate the κ discontinuity [28,29]. Such an approach is particularly interesting as the value of $\kappa \propto I_{\text{inj}}$ (current through injectors) and can be tuned during experiment [28,29].

In fact, two types of fractional vortices may exist in a 0-κ LJJ: a *direct* $-\kappa$ vortex, and a *complementary* $2\pi - \kappa$ vortex [29]. The "smaller" vortex corresponds to the ground state of the system, while the "bigger" one to the excited state. In the case $\kappa = \pi$, both vortices correspond to mirror symmetric semifluxons with a doubly degenerate ground state. Note, that the fluxon ($\kappa = 2\pi$) is an excited state of the system, with a constant phase being the ground state. Only using topological protection, e.g., an annular LJJ, one can trap the fluxon reliably.

While, being a soliton, the fluxon may freely move along the LJJ under the action of various forces (driving, friction, magnetic field gradient), the fractional vortex can only bend or deform, but it always stays in the vicinity of the 0-κ boundary. When the forces are released, the fractional vortex recovers its equilibrium shape, performing decaying oscillations around the equilibrium position [30], provided the system is underdamped.

It is crucial to know the eigenfrequencies of a fractional vortex. First, any classical device, which uses fractional vortices, should not operate at frequencies in the vicinity of the eigenfrequency (parasitic resonance). Second, an eigenfrequency gives hints about the stability of certain vortex configurations, namely, a low eigenfrequency is a clear sign that the system is close to an instability region; i.e., it may be sensitive to thermal noise, etc. Third, in the quantum domain, the eigenfrequency ω_0 defines the attempt frequency for macroscopic quantum tunneling, while, $\hbar\omega_0$ defines the energy gap between the ground state and the first excited (plasmon) state in the system.

In this Letter we report on the first experimental investigation of the eigenfrequency of a fractional Josephson vortex. Using microwave spectroscopy we measure the eigenfrequency as a function of κ (or the flux Φ carried by the vortex) and applied bias current (which deforms the vortex and changes its eigenfrequency).

The eigenfrequency ω_0 of a single fractional vortex in an infinite 0-κ LJJ at zero normalized bias current $\gamma = I/I_{c0} = 0$ and vanishing damping $\alpha = 0$ is [30]

$$\omega_0(\kappa, 0) = \omega_{p0}\sqrt{\frac{1}{2}\cos\frac{\kappa}{4}\left(\cos\frac{\kappa}{4} + \sqrt{4 - 3\cos^2\frac{\kappa}{4}}\right)}. \quad (1)$$

Here $I_{c0} = j_c wL$ is the "intrinsic" critical current, w and L are the width and length (circumference) of the LJJ, and j_c is the critical current density. In Eq. (1) the prefactor $\omega_{p0} = \sqrt{2\pi j_c/(\Phi_0 C)}$ is the intrinsic zero bias plasma frequency related to specific capacitance C of the Josephson barrier and j_c. For $\gamma \neq 0$ the analytical expression for $\omega_0(\kappa, \gamma)$ is unknown, but one can approximate it as

$$\omega_0(\kappa, \gamma) \approx \omega_0(\kappa, 0)\sqrt[4]{1 - \left(\frac{\gamma}{\gamma_c(\kappa)}\right)^2}, \quad (2)$$

where

$$\gamma_c(\kappa) = \frac{I_c(\kappa)}{I_{c0}} = \frac{I_c(\kappa)}{j_c wL} = \frac{\sin(\kappa/2)}{\kappa/2}, \quad (3)$$

is the normalized critical current of the junction (depinning current of the fractional vortex) at given κ [23,31,32]. Approximation (2) follows the same functional dependence as the plasma frequency of a small JJ [33,34]

$$\omega_p(\gamma) = \omega_{p0}\sqrt[4]{1 - \gamma^2}; \quad (4)$$

i.e., Eq. (2) is exact for $\kappa = 0$. It will serve as a guide for planning and performing the experiment.

For the experiments we used tunnel Nb-AlO_x-Nb annular LJJ (ALJJ) equipped with two pairs of current injectors as shown in Fig. 1. The tunnel ALJJ has low damping and allows us to perform resonant excitation of the fractional vortices and perform spectroscopy. The annular geometry, where the total topological charge is fixed, prevents flipping of a direct vortex to a complementary one with emission of a fluxon. Even if this happens, upon reset to the zero voltage state, the fluxon will be reabsorbed, turning the vortex into the initial state. Using the injectors we can change the value of κ during experiment and investigate $\omega_0(\kappa)$ (see below).

The ALJJ has a mean radius $R = 30$ μm, the width of the injectors and the distance between them are 5 μm. The Josephson penetration depth $\lambda_J \approx 43$ μm was estimated taking into account the idle region [35]. The normalized length of the ALJJ, thus, is $\ell \approx 4.35$.

Injectors are used to create a phase "discontinuity" κ on the length scale $\ll \lambda_J$. The short section of the top electrode between points A and B in Fig. 1 has an inductance $L_{\rm inj}$. A current $I_{\rm inj}$ passing through the inductance $L_{\rm inj}$ creates a phase drop $\kappa = L_{\rm inj} I_{\rm inj} 2\pi/\Phi_0$ across the short distance AB, i.e., the κ discontinuity. To calibrate injectors we have measured the critical current I_c as a function of $I_{\rm inj}$ for the left injector pair in Fig. 1. This $I_c(I_{\rm inj})$ is presented in Fig. 2 and looks like a perfect Fraunhoffer pattern in accord with the theory (3) [23,31,32]. The first minimum at $I_{\rm inj}^{\rm min} \approx \pm 6.92$ mA corresponds to $\kappa = \pm 2\pi$. Thus, for any $I_{\rm inj}$, the corresponding value of κ can be calculated as $\kappa = 2\pi I_{\rm inj}/|I_{\rm inj}^{\rm min}|$.

The measurements of the eigenfrequency were performed using resonant excitation of the fractional vortex by microwaves as follows. We apply a microwave radiation of fixed frequency $\omega_{\rm ex}$ and power P to our 0-κ ALJJ with a κ vortex. Then we ramp the bias current I from zero up to above I_c and observe at which current I_1 our ALJJ switches to nonzero voltage. Since, according to Eq. (2), the eigenfrequency decreases with the bias current, by ramping I one may reach the resonant condition $\omega_0(\kappa, \gamma) = \omega_{\rm ex}$ at some $\gamma_1 = I_1/I_{c0}$. The fractional vortex will be resonantly excited and will switch the ALJJ to the voltage state. In fact, we have been ramping the bias current many times, and have measured the escape histogram, which represents the probability of switching to the voltage state as a function of bias current γ; see Figs. 3(a) and 3(b). These

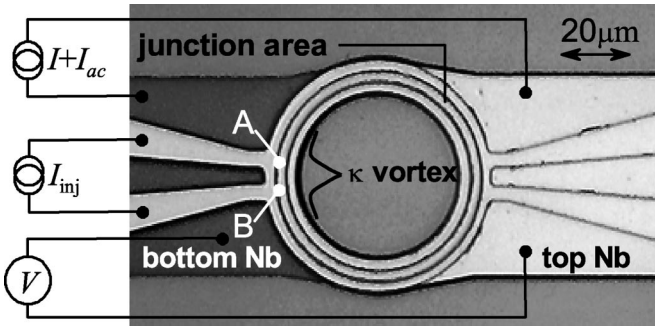

FIG. 1. Optical image (top view) of the investigated sample: ALJJ with two pairs of injectors. The phase discontinuity $-\kappa$, created by injectors induces a κ vortex. The microwaves induce ac current $I_{\rm ac}$ in the bias leads which adds up with the dc bias current I supplied by the current source.

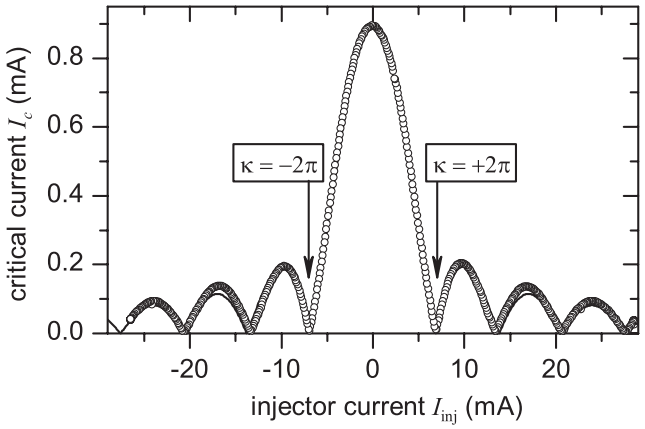

FIG. 2. The dependence $I_c(I_{\rm inj})$ measured at $T \approx 4.2$ K (symbols) and corresponding theoretical curve (continuous line).

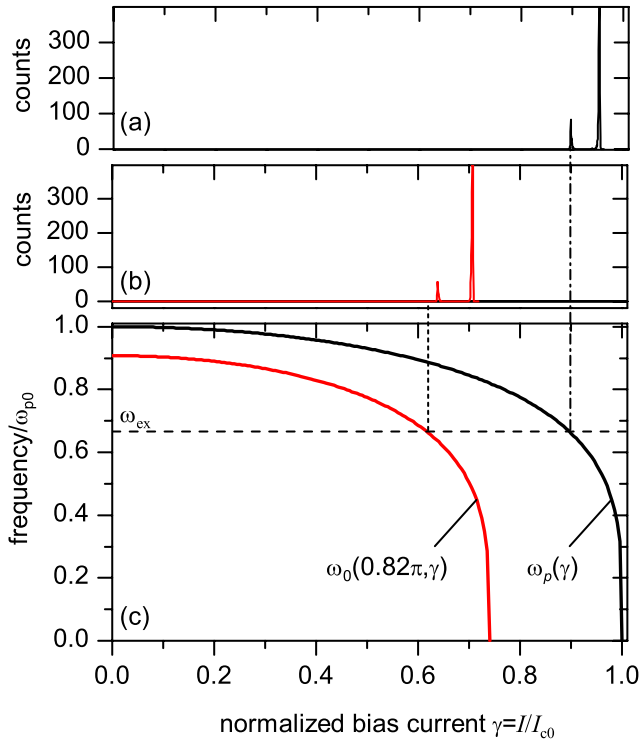

FIG. 3 (color online). Principle of the measurements. The escape histogram measured at $\omega_{ex}/2\pi = 29$ GHz (a) for $\kappa = 0$, i.e., $\omega_p(\gamma) = \omega_0(0, \gamma)$ and (b) for fractional vortex $\kappa = 0.82\pi$. The histograms show two peaks corresponding to resonant escape and thermal activation. (c) shows the numerically simulated dependences $\omega_0(0.82\pi, \gamma)$ (2) and $\omega_p(\gamma)$ (4). Applied frequency ω_{ex} is shown by the horizontal line.

histograms typically have two peaks. The first peak (at smaller I) at the intersection of $\omega_0(\kappa, \gamma)$ and ω_{ex} [Fig. 3(c)] corresponds to the resonant excitation of the phase $\mu(x)$ (in our case fractional vortex or phase-particle from the tilted washboard potential [34]) by microwaves. The second peak (at larger I) corresponds to the thermally activated escape of the Josephson phase from the potential well when the well becomes very shallow at I approaching $I_c(\kappa)$, see Refs. [33,34] for discussion of thermal escape in pointlike JJ. Note, that the critical current of our ALJJ depends on κ as described by Eq. (3) and shown in Fig. 2. The shape of thermal escape peak depends on the bias current ramp rate, on the bath temperature T and on the electronic noise [36]. Higher T leads to a broader peak shifted towards lower currents, which obscures the resonant activation peak especially for low ω_{ex} (high γ). The electronic noise has, to the first order, the same effect as the increase of T. Therefore, our setup was optimized as described below to keep the broadening caused by the electronic noise below the one caused by T.

The power P of the applied microwaves was kept as low as possible, but such that the first peak in the histogram is still visible. By increasing P the height of the first peak increases, but its position shifts due to the nonlinearity of the resonance. Accordingly, the height of the second peak decreases and it also shifts to lower γ. Measurements turned out to be easier at lower power and large γ when the particle is in the shallow well and both peaks are close. On the other hand, to resonantly excite the particle from the deep well (small γ), high power, which leads to nonlinear effects, is needed. Therefore the measurement results for high ω_{ex} (low γ) are not so accurate as for low ω_{ex} (high γ). The measurement technique and setup are similar to those described in Ref. [37].

Before measuring the eigenfrequency of a vortex and comparing it with the theory, we have to measure the plasma frequency ω_{p0} and I_{c0} with reasonable accuracy. To do this we excite our system by microwaves and make escape measurements at $I_{inj} = \kappa = 0$. In this case the ground state of the system corresponds to a uniform phase $\mu(x) = \arcsin(\gamma)$ and the lowest eigenfrequency is the plasma frequency $\omega_p(\gamma)$, Eq. (4), corresponding to spatially uniform oscillations (like in a pointlike junction). Formally, the plasma frequency is the eigenfrequency of a κ vortex with $\kappa = 0$, i.e., $\omega_p(\gamma) = \omega_0(0, \gamma)$. Escape histograms were measured for different ω_{ex} (with $I_{inj} = \kappa = 0$) and the position of the first peak $I_1(\omega_{ex})$ was, after inverting from $I_1(\omega_{ex}) = I_1(\omega_p)$ to $\omega_p(I_1)$, fitted using the theoretical dependence $\omega_p(\gamma)$ (4) as shown in Fig. 3(c). The fitting gives $\omega_{p0}/2\pi = 42.73$ GHz and a noise free $I_{c0} = 961$ μA. Note that I_{c0} represents the value of j_c most accurately. The critical current $I_c = I_s^{max} = 936$ μA measured from the thermal escape peak without microwaves represents the maximum supercurrent and has a somewhat lower value because of the slightly nonuniform current distribution in our ALJJ geometry. The critical current $I_c^{IVC} = 895$ μA measured from the I-V characteristic (IVC) or from $I_c(I_{inj})$ at $I_{inj} = 0$ (Fig. 2) is even lower.

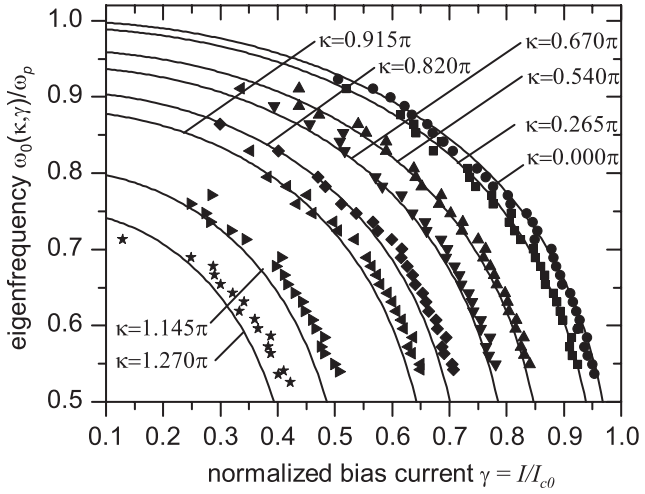

FIG. 4. Comparison between the theoretical curves with measurements of the eigenfrequency.

An independent numerical study of a microwave driven pointlike Josephson junction predicts that the position of the first peak is somewhat below the plasma resonance [38] calculated using Eq. (4). For a LJJ the situation may be even more complicated as the effective 1D potential may depend on various parameters, e.g., externally applied magnetic field [39] or trapped flux. For an ALJJ there are no theoretical calculations or numerical simulations so far. In this work we assume that $\omega_p(\gamma)$ is well described by Eq. (4) even for an ALJJ.

To measure the eigenfrequency of a κ vortex we repeated escape measurements for $\kappa \propto I_{\mathrm{inj}} > 0$. We have measured many escape histograms for a range of ω_{ex} and I_{inj} (i.e., κ), and were able to plot $\omega_0(\kappa, I)$. Knowing ω_{p0} and I_{c0} from the plasma frequency measurements we have plotted the dependence $\omega_0(\kappa, \gamma)$ in normalized units in Fig. 4. The theoretical curves $\omega_0(\gamma)$ at different κ are shown for comparison. To simulate them, we first numerically solved the sine-Gordon equation for an ALJJ with injectors of finite width to find the static state of the system. Then, to find the eigenfrequency, we have solved the associated eigenvalue problem numerically and, among all eigenfrequencies, selected the lowest positive one (imaginary part of eigenvalue).

Figure 4 shows that the experimental results are in good agreement with the theoretical predictions. Comparing the simulation results for finite injector sizes with the ones for ideal (pointlike) injectors, we saw that the eigenfrequency in Fig. 4 shifts towards larger γ (or ω_0 increases for fixed γ) as injectors get larger. Although we have included the geometrical dimensions of our injectors in simulations presented in Fig. 4, one can see that the experimental points are still somewhat shifted towards larger γ. This indicates that the effective injector size is larger than its geometric size.

We note that for low values of γ in Fig. 4 the accuracy of our measurements is limited by nonlinear effects. For large γ (low ω_{ex}) the measurements are limited by the thermal width of the peaks in the escape histogram. To study $\omega_0(\kappa, \gamma)$ for $\gamma \rightarrow 1$ we are going to perform the same measurements at $T < 4.2$ K.

In summary, we have performed spectroscopy of the fractional vortex eigenfrequency $\omega_0(\kappa, \gamma)$ in an annular long Josephson tunnel junction. The agreement of our results with the model confirms the concept of an artificial vortex with tunable fractional flux pinned at the phase discontinuity. This opens up new possibilities for further experimental studies of vortex molecules and fractional vortex crystals where one expects tunable splitting of eigenfrequencies [30] and tunable plasmonic band structure [26], accordingly.

We are grateful to the group of Professor A. Ustinov (especially to A. Kemp) from University of Erlangen for sharing their experience and numerous suggestions for improving the escape measurements setup as well as to M. Brendle for the help with the measurement electronics. This work is supported by the ESF program AQDJJ, by the DFG (Projects No. GO-1106/1 and No. SFB/TR-21), and by the Eliteförderprogramm of the Landesstiftung Baden-Württemberg.

*Electronic address: gold@uni-tuebingen.de

[1] A. Barone *et al.*, *Physics and Application of the Josephson Effect* (John Wiley & Sons, New York, 1982).
[2] K. K. Likharev, *Dynamics of Josephson Junctions and Circuits* (Gordon and Breach, Philadelphia, 1986).
[3] A. V. Ustinov, Physica (Amsterdam) **D123**, 315 (1998).
[4] V. P. Koshelets *et al.*, Rev. Sci. Instrum. **71**, 289 (2000).
[5] A. Kemp *et al.*, Phys. Status Solidi B **233**, 472 (2002).
[6] Arbitrary fractional vortices may also appear in a LJJ with a strong second harmonic in the current-phase relation, which can be present either intrinsically or due to frequently alternating regions of negative and positive critical current. In contrast to such ''splintered'' vortices [7,8], the fractional vortices discussed here are pinned at the 0-κ boundary.
[7] R. G. Mints *et al.*, Phys. Rev. Lett. **89**, 067004 (2002).
[8] R. Mints, Phys. Rev. B **57**, R3221 (1998).
[9] J. R. Kirtley *et al.*, Science **285**, 1373 (1999).
[10] H. Hilgenkamp *et al.*, Nature (London) **422**, 50 (2003).
[11] J. R. Kirtley *et al.*, Phys. Rev. B **72**, 214521 (2005).
[12] L. N. Bulaevskii *et al.*, Solid State Commun. **25**, 1053 (1978).
[13] J. H. Xu *et al.*, Phys. Rev. B **51**, 11 958 (1995).
[14] E. Goldobin *et al.*, Phys. Rev. B **66**, 100508(R) (2002).
[15] D. J. Van Harlingen, Rev. Mod. Phys. **67**, 515 (1995).
[16] M. L. Della Rocca *et al.*, Phys. Rev. Lett. **94**, 197003 (2005).
[17] S. M. Frolov *et al.*, Phys. Rev. B **74**, 020503 (2006).
[18] M. Weides *et al.*, Phys. Rev. Lett. **97**, 247001 (2006).
[19] V. G. Kogan *et al.*, Phys. Rev. B **61**, 9122 (2000).
[20] A. Zenchuk *et al.*, Phys. Rev. B **69**, 024515 (2004).
[21] H. Susanto *et al.*, Phys. Rev. B **68**, 104501 (2003).
[22] J. R. Kirtley *et al.*, Phys. Rev. B **56**, 886 (1997).
[23] E. Goldobin *et al.*, Phys. Rev. B **70**, 094520 (2004).
[24] N. Lazarides, Phys. Rev. B **69**, 212501 (2004).
[25] E. Goldobin *et al.*, Phys. Rev. B **67**, 224515 (2003).
[26] H. Susanto *et al.*, Phys. Rev. B **71**, 174510 (2005).
[27] E. Goldobin *et al.*, Phys. Rev. B **72**, 054527 (2005).
[28] E. Goldobin *et al.*, Phys. Rev. Lett. **92**, 057005 (2004).
[29] E. Goldobin *et al.*, Phys. Rev. B **70**, 174519 (2004).
[30] E. Goldobin *et al.*, Phys. Rev. B **71**, 104518 (2005).
[31] C. Nappi *et al.*, Phys. Rev. B **65**, 132516 (2002).
[32] B. A. Malomed *et al.*, Phys. Rev. B **69**, 064502 (2004).
[33] T. A. Fulton *et al.*, Phys. Rev. B **9**, 4760 (1974).
[34] M. H. Devoret *et al.*, Phys. Rev. Lett. **53**, 1260 (1984).
[35] R. Monaco *et al.*, J. Appl. Phys. **77**, 2073 (1995).
[36] P. Silvestrini *et al.*, Phys. Rev. B **37**, 1525 (1988).
[37] A. Wallraff *et al.*, Rev. Sci. Instrum. **74**, 3740 (2003).
[38] N. Grønbech-Jensen *et al.*, Phys. Rev. Lett. **93**, 107002 (2004).
[39] M. G. Castellano *et al.*, Phys. Rev. B **54**, 15 417 (1996).